Rescue of Exhausted CD8 T cells by PD-1 Targeted Therapies is CD28-dependent

Alice O. Kamphorst, Andreas Wieland, Tahseen Nasti, Shu Yang, Ruan Zhang, Daniel L. Barber, Bogumila T. Konieczny, Candace Z. Daugherty, Lydia Koenig, Ke Yu, Gabriel L. Sica, Arlene H. Sharpe, Gordon J. Freeman, Bruce R. Blazar, Laurence A. Turka, Taofeek K. Owonikoko, Rathi Pillai, Suresh S. Ramalingam, Koichi Araki, Rafi Ahmed[*]

*correspondence to: rahmed@emory.edu

This PDF file includes:

> Materials and Methods
> Supplementary References
> Figs. S1 to S9

Materials and Methods

NSCLC patient samples:

Institutional review board approval was obtained prior to study enrollment and written informed consent was obtained from all donors. For blood samples collections, we approached NSCLC patients treated at Winship Cancer Institute who were initiating therapy with anti-PD-1 or anti-PD-L1 blocking antibodies on clinical trials or as standard of care therapy to participate in our study. Patients received anti-PD-1 therapy pembrolizumab/MK-3475 (10 mg/kg) or nivolumab (3mg/kg), or anti-PD-L1 therapy MPDL3280A (atezolizumab) (1200mg) as intravenous infusion every 2-3 weeks until disease progression or unacceptable side effect. Peripheral blood samples were collected before infusion (baseline) and at second treatment into cell preparation tubes with sodium citrate (BD). Peripheral blood mononuclear cells were isolated according to standard protocol and immediately stained or frozen for posterior analysis. Lung tumor specimens were obtained from 17 patients with NSCLC that underwent surgical resection as standard care. Samples collected were comprised of 4 squamous cell carcinomas (stage II-III) and 13 adenocarcinomas (stage IA-IV). Tumors were harvested in cold L-15 Leibovitz media (HyClone), minced into small pieces and digested for 1h at 37°C with shaking with an enzymatic cocktail of Collagenase I (125mg/1L), DNase I (50mg/1L), Collagenase IV (125mg/1L), Collagenase II (125mg/1L), Elastase (50mg/1L) (Worthington). Single cell suspensions were obtained, and after RBC ACK lysis, cells were stained for immediate analysis by flow cytometry.

Mice and infections:

C57BL/6, Balb/c, B6 CD45.1, CD28KO and $Rosa26^{Cre-ERT2}$ mice were purchased from the Jackson Laboratory. CD28KO were bred to CD45.1 P14 TCR transgenic mice in house. $Rosa26^{Cre-ERT2}$ mice were bred to CD28$^{f/f}$ mice (27), and CD45.1 P14 TCR transgenic mice in house. Mice were infected at 6-8 weeks of age and mixed bone marrow chimera mice were infected 8-12 weeks after irradiation and reconstitution. For acute LCMV infection mice were given $2x10^5$ plaque forming units (PFU) LCMV Arm by intraperitoneal route (i.p.). For chronic LCMV infection mice were given 500 μg of the CD4-depleting antibody GK1.5 i.p. (BioXcell) 1 day prior to infection and again on the day of infection with $2x10^6$ PFU LCMV clone 13 by intravenous route (i.v.) (9). Mice were analyzed 45 to 95 days post-infection. Viral load was assayed by plaque assays on Vero E6 cells as previously described (28). All mice were used in accordance with the Emory University Institutional Animal Care and Use Committee Guidelines.

Adoptive cell transfers:

For experiments using P14 T cells, 1-2 days before infection, $2\text{-}5 \times 10^3$ P14 T cells were transferred i.v. Cell transfer consisted of CD8 T cell-enriched fraction (CD8 T cell isolation kit, Miltenyi Biotec) or total splenocytes isolated from naïve P14 mice. In co-transfer experiments of CD28KO and WT P14, 3-4 fold more CD28KO cells were transferred to achieve a 1:1 KO to WT ratio in chronically infected mice.

For mixed bone marrow chimera experiments, recipient mice (at least 8-week old) received one dose of 550 rad. Bone marrow cells were isolated from donor mice and

prepared into single cell suspensions. 5-10 x10^6 bone marrow cells depleted of CD4 and CD8 T cells (Milteny Biotec) were transferred i.v. and mice were rested for 2-3 months to allow for reconstitution before infection.

In vivo tumor model:

Balb/c mice were inoculated subcutaneously with 0.2 x 10^6 CT26 colon carcinoma cells in 25% matrigel and depleted of CD4 T cells by i.p. injection of 250 μg GK1.5 antibody. (BioXcell). CD4 depletion was maintained for the duration of the experiment by repeated injections of 250 μg GK1.5 antibody every 7-10 days. CD4 depletion was performed to restrict our study on CD8 T cells and avoid potential effects on CD4 Treg cells by B7-blocking antibodies that would interfere with interpretation of the results (*29*). Mice were randomized into different treatment groups when CT26 tumor reached 150 mm^3 (±70mm^3), between 11-14 days after inoculation. Mice whose tumors exceeded acceptable limits (19 mm^3 diameter or ulcerated tumors) were euthanized and removed from the study. Tumors were measured every 2-4 days using a caliper and tumor growth was calculated as volume of ellipsoid (length x width x height x 0.52).

In vivo treatments:

For blockade of the PD-1 pathway, 200 μg anti-mouse PD-L1 antibody (10F.9G2, prepared in house) or 200 μg anti-mouse PD-1 antibody (29F.1A12, prepared in house) was administered i.p. every 3 days.. Where indicated we also treated mice with 200 μg anti-mouse-PD-1 clone muDX400 (Merck), administered i.p. every 3-5 days. For

blockade of B7 molecules, 500 μg CTLA-4-Ig or 200 μg anti-mouse B7-1 (16-10A1, BioXcell) and 200 μg anti-mouse B7-2 (GL-1, BioXcell) were administered i.p. a few hours before the first dose of anti-PD-L1 or anti-PD-1, and then every 3 days. Final analyses were performed 14 days after treatment initiation, unless indicated otherwise.

In vivo conditional CD28 gene deletion was achieved in *Rosa26*[Cre-ERT2] CD28[f/f] cells by tamoxifen administration to LCMV chronically infected mice. Tamoxifen (Sigma-Aldrich) was dissolved in ethanol, diluted 1:20 in sunflower oil, and sonicated for 5 min at 37°C. Mice were injected daily with 1 mg tamoxifen i.p. for 5 consecutive days, then rested for a minimum of 7 days before further treatment.

Antibodies and flow cytometry:

Human samples: Peripheral blood mononuclear cells were stained with anti-CD8 (RPA-T8), -CD4 (RPA-T4), -CD3 (UCHT1), -CD45RA (2H4LDH11LDB9), -CCR7 (150503), -PD-1 (EH12.2H7), -CD28 (CD28.2), -HLA-DR (l243), -CD38 (HIT2) and -Ki67 (B56). After anti-PD-1 treatment, PD-1 expression was detected by combining anti-human IgG4 biotin (HP-6025, Sigma) with anti-PD-1 antibody. Live/Dead cell discrimination was performed using fixable Yellow Dead Cell Stain Kit (Life Technology). Intracellular staining for Ki-67 was performed using Foxp3 Fixation Kit (eBioscience). Antibodies were purchased from BD Bioscience, Biolegend, eBioscience or Beckman Coulter. Single cell suspensions obtained from lung tumor were stained with anti-CD8 (RPA-T8), -CD4 (RPA-T4), -CD3 (UCHT1), -PD-1 (EH12.2H7), -CD28 (CD28.2) from BD or

Biolegend; anti-TIM-3 (344823) from R&D. Live/Dead cell discrimination was performed using fixable Yellow Dead Cell Stain Kit (Life Technology).

Murine tissues: Single cell suspensions were obtained from blood, spleen, lung and liver as previously described (*29*). Single cell suspensions were stained with anti-CD8α (53-6.7), -CD4 (RM4-5), -CD45.1 (A20), -CD45.2 (104), -CD44 (IM7), anti-CD28 (E18) and -PD-1 (RMP1-30 or 29F.1A12) from BD, eBioscience or Biolegend; TIM-3 (215008) from R&D systems. Dead cells were excluded by gating out cells positive for Live/Dead fixable dead cell stain (Invitrogen). LCMV MHC class I tetramers were prepared and used as previously described (*30*). LCMV-specific responses were assessed by re-stimulating splenocytes with 0.1 μg/ml of GP33, GP276, NP396, NP118 or NP235 LCMV peptides in the presence of GolgiPlug (brefeldin A) and GolgiStop (monesin) for 5h at 37°C. Intracellular staining for IFN-γ (XMG1.2), TNF-α (MP6-XT22), and granzyme B (GB12 or GB11) was performed with Cytofix/Cytoperm kit (BD Biosciences). Intracellular staining for Ki-67 (B56, BD Pharmingen) was performed with Foxp3/ Transcription Factor Staining Buffer Set (eBioscience) according to manufacturer's instructions.

Samples were acquired with a Becton Dickinson FACS Canto or LSRII and analyzed using FlowJo (Treestar).

Statistical analysis:

All data were analyzed using Prism 6 (GraphPad).

Supplementary References

27. R. Zhang *et al.*, An obligate cell-intrinsic function for CD28 in Tregs. *J Clin Invest* **123**, 580-593 (2013).

28. R. Ahmed, A. Salmi, L. D. Butler, J. M. Chiller, M. B. Oldstone, Selection of genetic variants of lymphocytic choriomeningitis virus in spleens of persistently infected mice. Role in suppression of cytotoxic T lymphocyte response and viral persistence. *J Exp Med* **160**, 521-540 (1984).

29. D. Masopust, V. Vezys, A. L. Marzo, L. Lefrancois, Preferential localization of effector memory cells in nonlymphoid tissue. *Science* **291**, 2413-2417 (2001).

30. E. J. Wherry, J. N. Blattman, K. Murali-Krishna, R. van der Most, R. Ahmed, Viral persistence alters CD8 T-cell immunodominance and tissue distribution and results in distinct stages of functional impairment. *J Virol* **77**, 4911-4927 (2003).
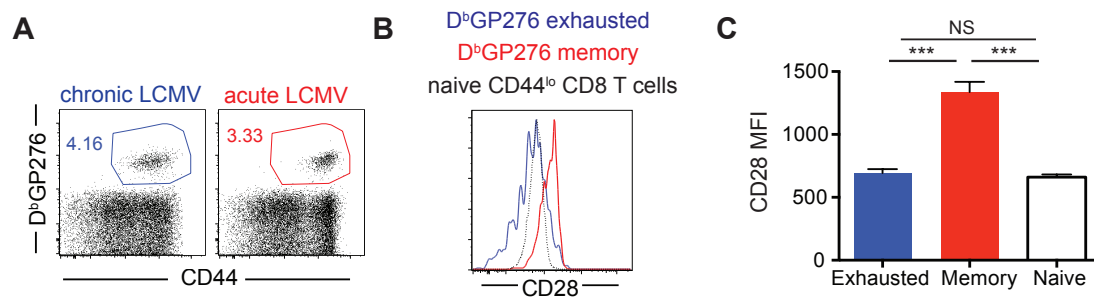
Fig. S1.

Exhausted CD8 T cells express similar levels of CD28 than naïve cells, but lower levels than memory CD8 T cells. C57BL/6 mice were infected with acute LCMV Arm or chronic LCMV clone13. Splenocytes were analyzed at least 45 days post-infection when CD8 T cells have differentiated into memory cells after acute infection or exhausted cells after chronic infection. (A) Gating on LCMV-D^{b}GP276-specific cells after gating on splenic CD8 T cells. Data are from representative mice from 4 independent experiments with 3-6 mice per group. (B) CD28 expression on memory (red) or exhausted (blue) LCMV-D^{b}GP276-specific CD8 T cells. Dashed black line shows CD28 expression on naïve CD44^{lo} CD8 T cells. Data are from representative mice from 4 independent experiments with 3-6 mice per group. (C) Mean fluorescence intensity as in B. Representative data from one experiment (N=3) out of 4 independent experiments. Error bars indicate SEM. ANOVA with Sidak's correction for multiple comparisons. ***P<0.001.. NS = not significant.

A

Chronic LCMV

αPD-L1 → analysis after 14d

B

D^{b}GP276

P = 0.82
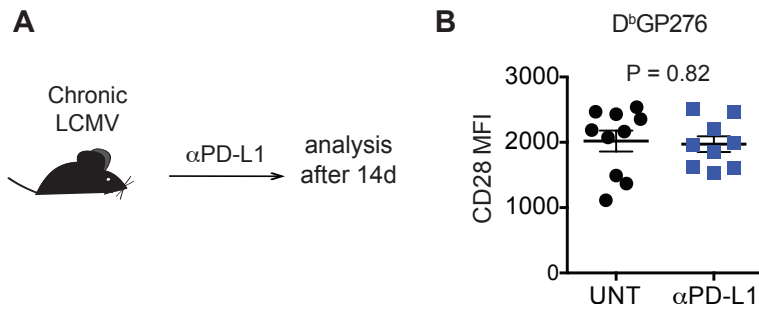
Fig. S2

Rescue by PD-1 therapy does not increase CD28 expression on LCMV-specific CD8 T

cells. (A) Experimental layout. (B) CD28 mean fluorescence intensity (MFI) on LCMV-

D^{b}GP276-specific CD8 T cells in the spleen of chronically infected mice. Data show

compiled data from two experiments and is representative from 4 independent

experiments with 3-5 mice per group. Error bars indicate SEM. Unpaired t-test.
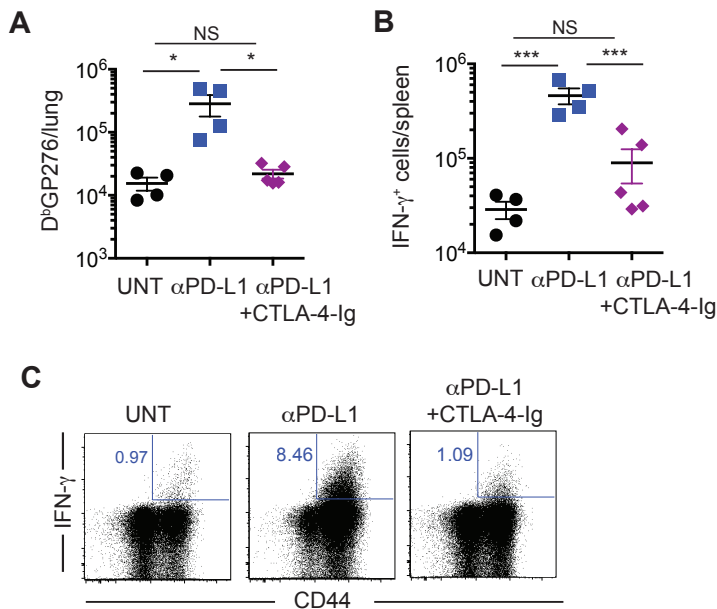
Fig. S3

CTLA-4-Ig abrogates anti-PD-L1-mediated rescue of exhausted CD8 T cells.

At least 45 days after establishment of chronic infection with LCMV clone 13, indicated

groups of mice were treated with anti-PD-L1 as a single agent or in combination with

CTLA-4-Ig. Analysis was performed after 14 days of treatment. (A) Number of LCMV-

D^bGP276-specific CD8 T cells in the lung. Data show one representative of 2

independent experiments, with at least 4 mice per group. Error bars indicate SEM. (B)

Number of IFN-γ–producing CD8 T cells in the spleen after *ex vivo* restimulation with

LCMV GP276 peptide. Data show one representative of 2 independent experiments, with

at least 4 mice per group. Error bars indicate SEM. (C) Frequencies of CD8 T cells

producing IFN-γ in the spleen after *ex vivo* restimulation with a pool of LCMV peptides.

Data show representative mice of 2 independent experiments, with at least 4 mice per

group. ANOVA with Sidak's correction for multiple comparisons. *P<0.05, ***P<0.001.

NS = not significant.
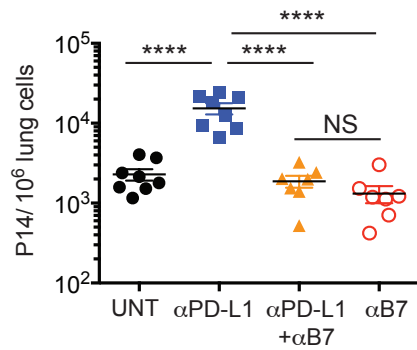
Fig. S4

Transient B7 blockade prevents rescue of LCMV-specific exhausted CD8 T cells by PD-1 therapy, but has no major impact on the maintenance of LCMV-specific exhausted CD8 T cells during chronic infection. Experiment layout as in Fig. 1K. Graph shows frequency of P14 cells in lung. Data show compilation of 2 independent experiments, with 3- 4 mice per group. ANOVA with Sidak's correction for multiple comparisons. Error bars indicate SEM. ****$P<0.0001$. NS = not significant.
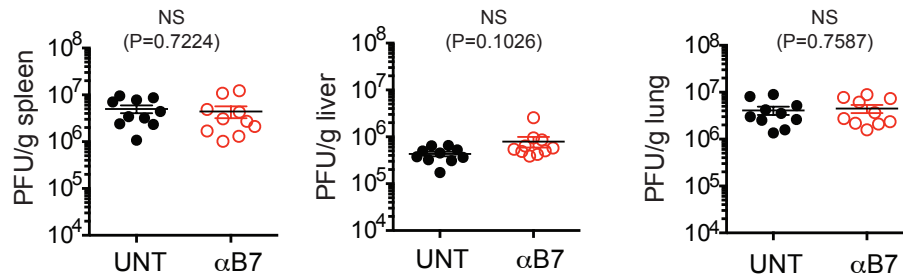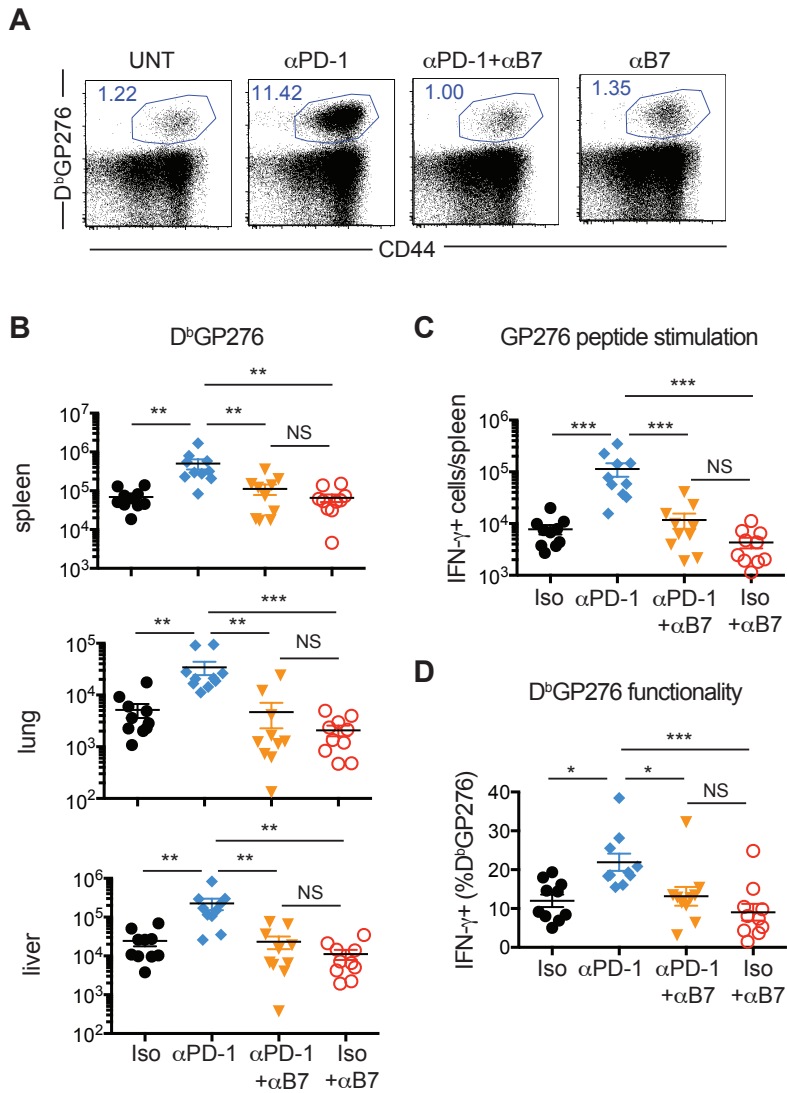
Fig. S5

Transient blockade of the B7-pathway in mice with established LCMV chronic infection does not affect viral load. Graphs show viral load in different organs after a two-week B7 blockade regimen in mice with established LCMV chronic infection (as in Fig. 1A). Data show compiled data from two independent experiments with 4-5 mice per group. Error bars indicate SEM. Unpaired t-test.
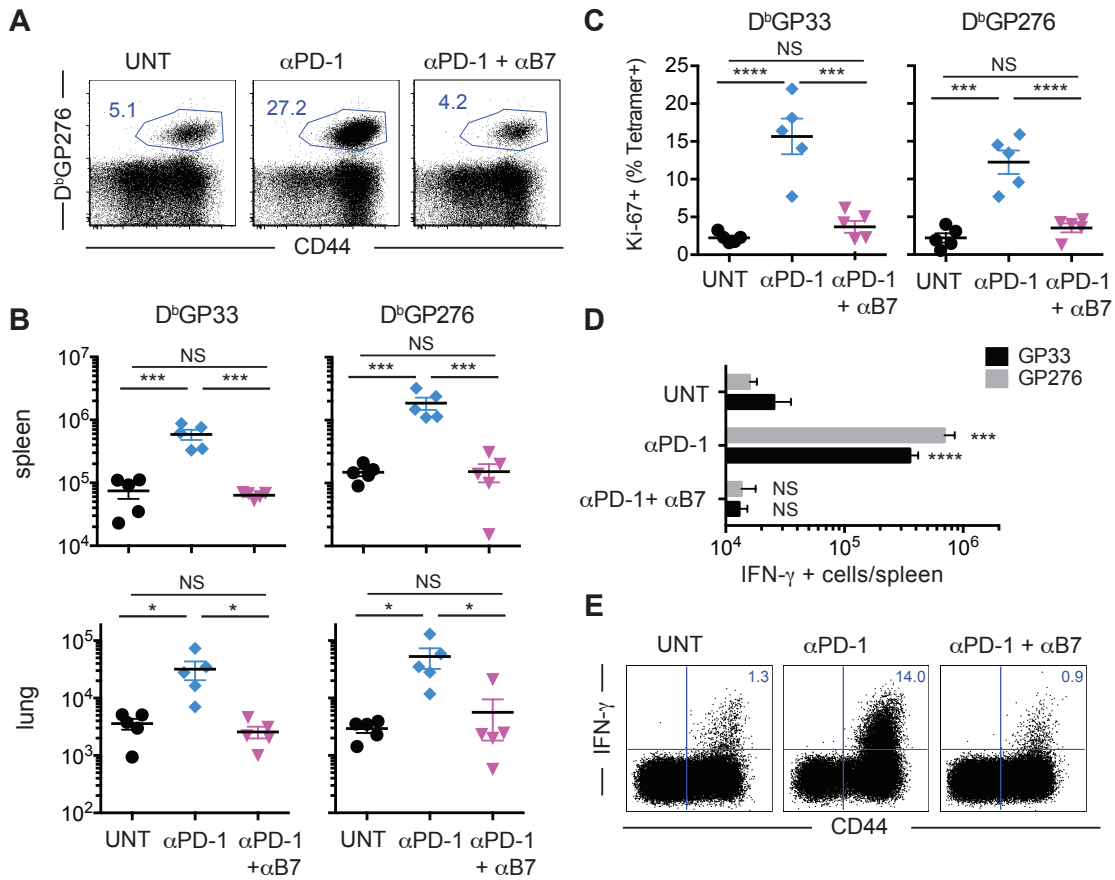
Fig. S6

CD8 T cell rescue by PD-1 therapy also relies on B7 costimulation. At least 45 days after establishment of LCMV clone 13 chronic infection, indicated groups of mice were treated for 2-weeks with anti-PD-1 (clone 29F.1A12, rat IgG2a) as a single agent or in combination with anti-B7-1 and anti-B7-2. (A) Frequencies of LCMV-D^{b}GP276-specific CD8 T cells in the spleen. Data show representative mice from 3 independent experiments with 4-5 mice per group. (B) Numbers of LCMV-D^{b}GP33 and LCMV-D^{b}GP276-specific CD8 T cells in different organs. Data show one representative experiment of 3 independent experiments with 4-5 mice per group. Error bars indicate SEM. (C) Ki-67 expression on LCMV-D^{b}GP33 and LCMV-D^{b}GP276-specific CD8 T

cells in the spleen. Data show one representative experiment of 2 independent experiments with 4-5 mice per group. Error bars indicate SEM. (D) Numbers of IFN-γ–producing CD8 T cells in the spleen after *ex vivo* restimulation with the indicated LCMV peptides. . Data show one representative experiment of 3 independent experiments with 4-5 mice per group. Comparisons are between treated groups and untreated mice. Error bars indicate SEM. (E) Frequencies of CD8 T cells producing IFN-γ in the spleen after *ex vivo* restimulation with a pool of LCMV peptides. Data show representative mice from 3 independent experiments with 4-5 mice per group. ANOVA with Sidak's correction for multiple comparisons. *P<0.05, ***P<0.001, ****P<0.0001. NS = not significant.

A

UNT   αPD-1   αPD-1+αB7   αB7

1.22   11.42   1.00   1.35

D^bGP276 — CD44

B D^bGP276

spleen — lung — liver

Iso   αPD-1   αPD-1 +αB7   Iso +αB7

C   GP276 peptide stimulation

IFN-γ+ cells/spleen

Iso   αPD-1   αPD-1 +αB7   Iso +αB7

D D^bGP276 functionality

IFN-γ+ (%D^bGP276)

Iso   αPD-1   αPD-1 +αB7   Iso +αB7

Fig. S7

B7-costimulation is required for CD8 T cell rescue by PD-1 therapy. At least 45 days

after LCMV clone 13 chronic infection, indicated groups of mice were treated for 2-

weeks with anti-PD-1 (clone muDX400, mouse IgG1), isotype control mouse IgG1 or

combination with anti-B7-1 and anti-B7-2 blocking antibodies. (A) Frequencies of

LCMV-D^bGP276-specific CD8 T cells in the spleen. Data show representative mice from

2 independent experiments with 4-5 mice per group. (B) Numbers of LCMV-D^bGP276-

specific CD8 T cells in different organs. Data show compiled data from 2 independent

experiments with 4-5 mice per group each. Error bars indicate SEM. (C) Numbers of

IFN-γ–producing CD8 T cells in the spleen after *ex vivo* restimulation with LCMV

GP276 peptide. Data show compiled data from 2 independent experiments with 4-5 mice

per group each. Error bars indicate SEM. (D) Frequencies of LCMV-D^{b}GP276-specific

CD8 T cells producing IFN-γ after *ex vivo* restimulation with LCMV GP276 peptide.

Data show compiled data from 2 independent experiments with 4-5 mice per group each.

Error bars indicate SEM. ANOVA with Sidak's correction for multiple comparisons.

*P<0.05, **P<0.01, ***P<0.001. NS = not significant.
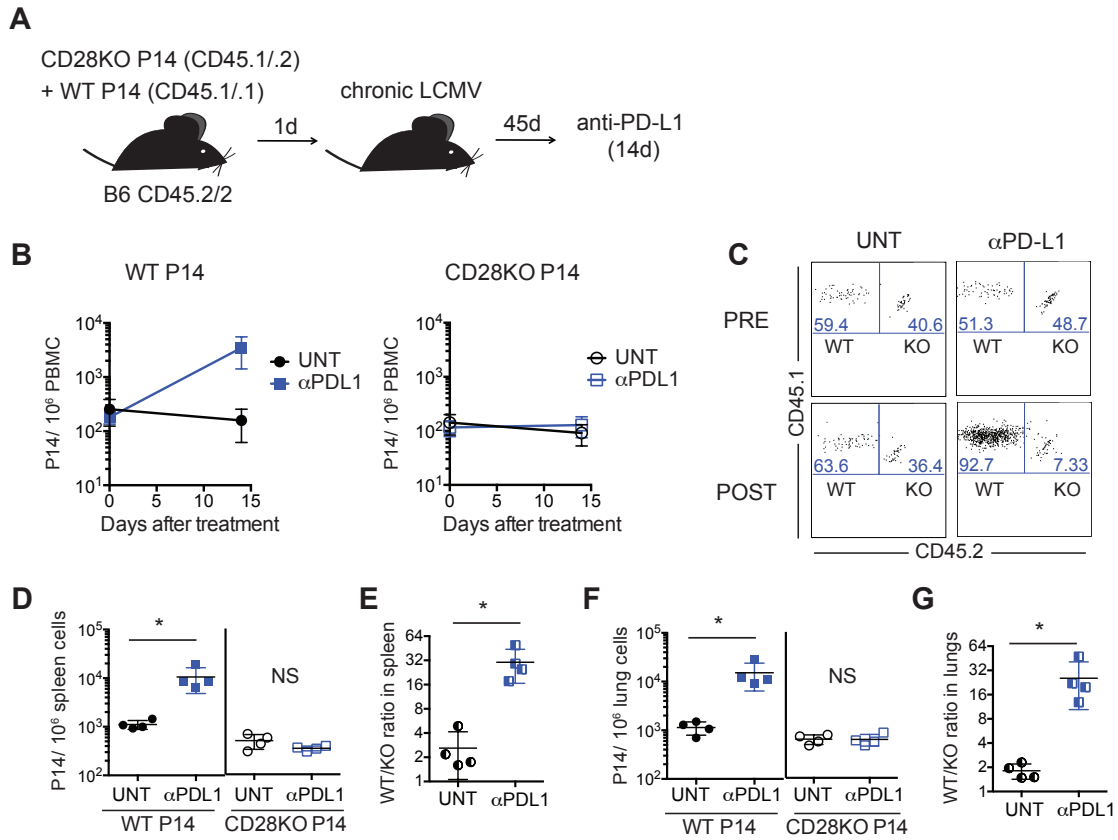
Fig. S8

CD28 deficient LCMV-specific CD8 T cells fail to expand following blockade of the PD-1 pathway during chronic infection. (A) Experiment layout. (B) Frequencies of P14 cells in blood pre and post anti-PD-L1 treatment. Data are from one representative experiment of 3 independent experiments, with at least 3 mice per group. Error bars indicate SEM. (C) Gating strategy to quantify WT and CD28KO P14 cells in blood. Data show representative mice, pre and post-treatment of data summarized in B. (D) Frequencies of P14 cells in spleen. Data are from one representative experiment of 3 independent experiments, with at least 3 mice per group. Error bars indicate SEM. (E) WT to CD28KO P14 ratio in the spleen. Data are from one representative experiment of 3

independent experiments, with at least 3 mice per group. Error bars indicate SEM. (F)

Frequencies of P14 cells in lung. Data are from one representative experiment of 3

independent experiments, with at least 3 mice per group. Error bars indicate SEM. (G)

WT to CD28KO P14 ratio in the lung. Data are from one representative experiment of 3

independent experiments, with at least 3 mice per group. Error bars indicate SEM. D and

F, Unpaired t-test, E and G, Mann Whitney test. *P<0.05. NS = not significant.
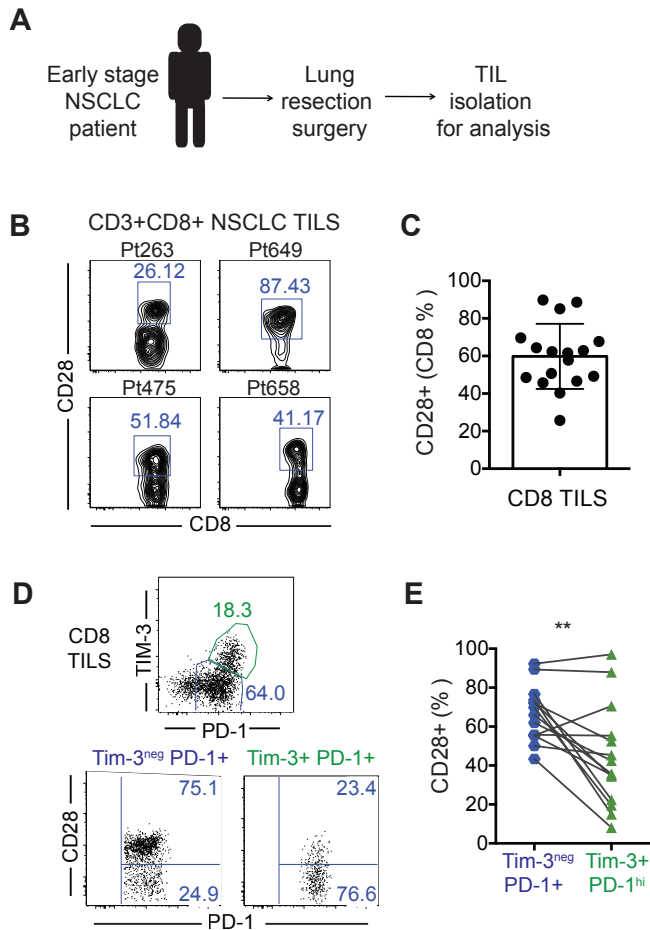
Fig. S9

CD28 expression on CD8 T cells infiltrating NSCLC tumors. (A) Study design (N=17).

(B) CD28 expression on CD8 TILs from 4 representative patients (Pt). (C) As, in B, but

graph shows data from all 17 patients. Error bars indicate SEM. (D) Gating on TIM-3^{neg}

PD-1+ and TIM-3+ PD-1+CD8 TILs, and expression of CD28 on those T cell subsets in

a representative tumor. (E) Summary of the data as in D (N=14, three tumor samples

containing less than 2% TIM-3+ cells among CD8 T cells were omitted from this

analysis). ** P<0.01 (Paired t-test).